Optical characterization of the Bi_2O_3, TiO_2 and MnO_2 doped ZnO Ceramics

ZAHID RIZWAN*, AZMI ZAKARIA, M. G. M. SABRI, FASHI UD DIN
Department of Physics, Faculty of Science, University Putra Malaysia, 43400 Serdang, Selangor D. E., Malaysia

Photopyroelectric (PPE) spectroscopy was used to study the optical band-gap energy (E_g) of the ceramic ZnO doped with $0.5MnO_2$. xBi_2O_3 and $xTiO_2$ sintered at 1270°C for one to four hours. The wavelength of incident light from 300 to 800 nm, modulated at 9 Hz, was used and PPE spectrum with reference to the doping level and sintering time was discussed. The optical band-gap energy (E_g) was determined from the plot $(\rho h\upsilon)^2$ vs $h\upsilon$ and found that the E_g decreased to the lowest value of 2.13 eV with x = 1.8 mol% at four hour sintering time. Steepness factor (in region-A) and steepness factor (in region-B) which characterizes the slope of exponential optical absorption was discussed with reference to the variation in the value of E_g. XRD, SEM and EDAX were used for the characterization of the ceramic. Relative density and grain size is also discussed.

(Received July 16, 2010; accepted April 11, 2011)

Keywords: Photopyroelectric Spectroscopy, Bi_2O_3, TiO_2, MnO_2, ZnO, Varistor

1. Introduction

ZnO is n-type semiconductor and used in manufacturing of paints, pharmaceuticals products, cosmetics, rubber, plastics, textiles, inks, batteries, etc. It is also used in electrical components such as phosphors, piezoelectric transducers, blue laser diodes, solar cell electrodes, gas sensors and varistor [1 2, 3,4]. The precise role of many dopants in the electronic structure of ZnO based varistor is indecisive. ZnO based varistor is formed with other metal oxides of small amounts such as Bi_2O_3, Co_3O_4, Cr_2O_3 MnO, Sb_2O_3, etc. Such dopants are the main tools that are used to enhance the non-linear response and the stability of ZnO based varistors [5]. The purpose of this paper is to study the effect of the variation of doping level of xBi_2O_3 and $xTiO_2$ (in the presence of $0.5MnO_2$) on photopyroelectric (PPE) signal intensity spectra. It is, therefore, important to study optical absorption behavior for investigating electronic states in this ceramic. In this study PPE spectroscopy, a powerful non-radiative tool [6], is used to investigate the optical absorption behavior for the ceramic ZnO doped with $0.5MnO_2$, xBi_2O_3, $xTiO_2$.

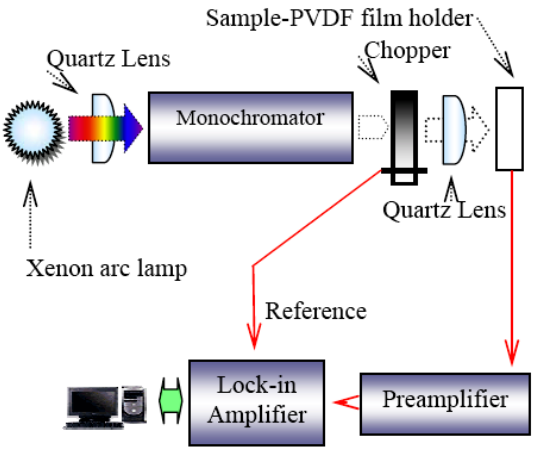

Fig. 1. Schematic diagram of experimental setup.

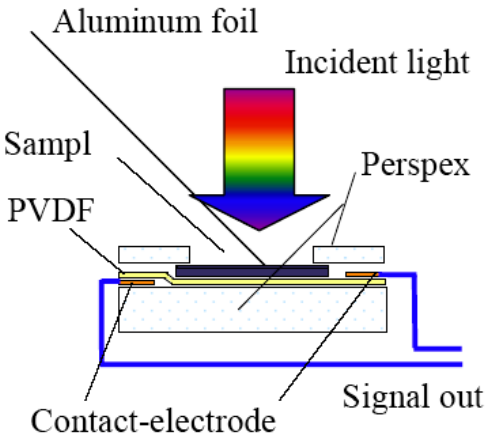

Fig. 2. Schematic diagram of sample PVDF sensor holder

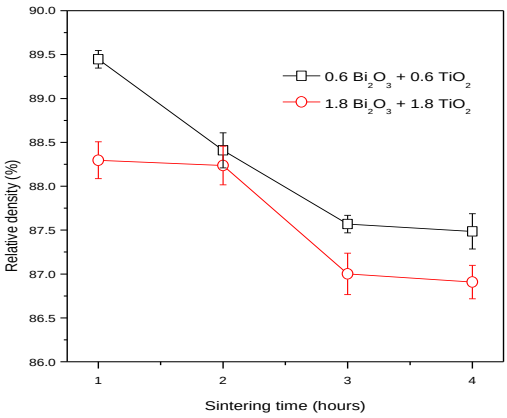

Fig. 3. Variation of density with sintering time

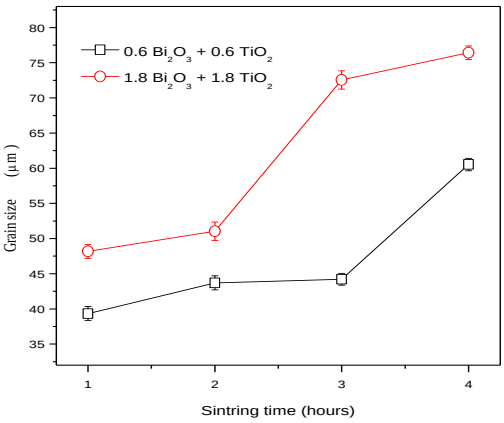

Fig. 4. Variation of grain size with sintering time

2. Materials and methods

ZnO (99.9% purity, Alfa Aesar) was doped with xBi_2O_3 (99.99 % purity, Alfa Aesar), $xTiO_2$ (99.99 % purity, Alfa Aesar) and $0.5MnO_2$ (99.99 % purity, Alfa Aesar) where x = 0.6, 1.8 mol%. The 22 hours ball milled powder of each mole percent was pre-sintered at temperatures 700°C for two hours in air. The heating and cooling rate was 4°C min^{-1}. Each sample was ground and polyvinyl alcohol (1.3 wt. %) was mixed as a binder to avoid cracks in samples. The dried powder was pressed under a force of 800 kg cm^{-1} to form a disk of 10 mm diameter with about one millimeter thickness. Finally the pellets were sintered at 1270°C for one, two, three and four hours in air at a heating and cooling rate of 6°C min^{-1} for the ceramics ZnO + 0.6 Bi_2O_3 + 0.6 TiO_2 + 0.5 MnO_2 and ZnO + 1.8 Bi_2O_3 + 1.8 TiO_2 + 0.5 MnO_2. The disk from each sample was ground for two hours and granulated by sieving through a 75-mesh screen for the PPE spectroscopy and XRD analysis. Density was measured by geometrical method taking the average of 12 disks. The surface of samples was prepared like mirror and samples were thermally etched for microstructure analysis and average grain size was determined by grain boundary-crossing method. Cu K_α radiation with PAN Analytical (Philips) X'Pert Pro PW1830 was used for X-ray diffraction studies and the XRD data were analyzed using X'Pert High Score software for the identification of crystalline phases developed in the ceramics.

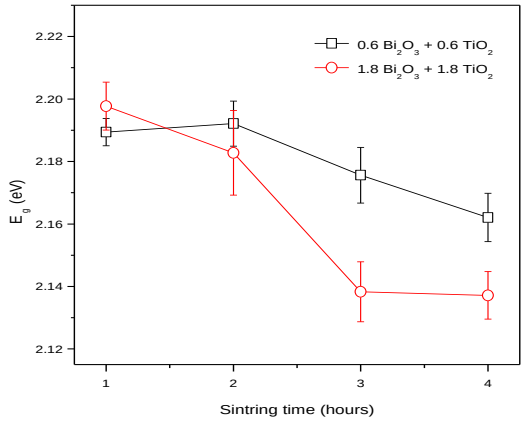

Fig. 5. Variation of E_g with sintering time

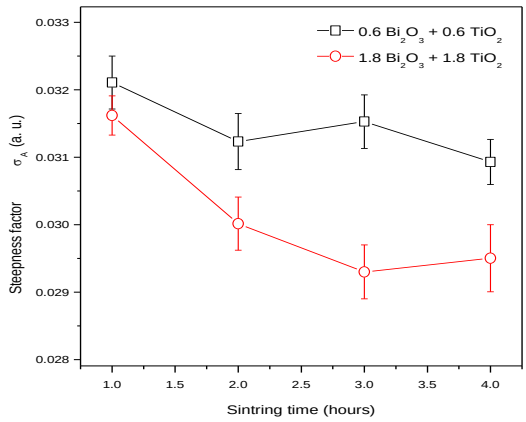

Fig. 6. Effect of sintering time on steepness factor (σ_A)

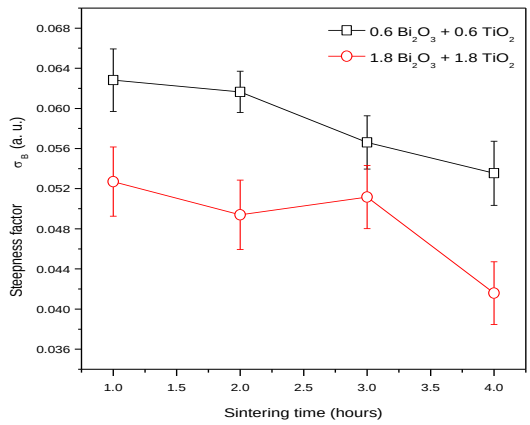

Fig. 7. Effect of sintering time on steepness factor (σ_B)

Measurement of PPE signal amplitude by PPE spectrometer has been described elsewhere [7]. For sample treatment prior to photopyroelectric measurement, fine powder was again ground in double deionized water. Few drops of each mixture were poured on an aluminum foil of area about 2 cm^2 and dried at room temperature to form a thin layer of sample on aluminum foil. The foil was placed in contact to a Polyvinylidene Fluoride (PVDF) PPE sensor using silver conductive grease between two Perspex plates (Fig. 2). One kW Xenon arc lamp (Oriel model 6269) was used in this study (Figure1). The range of the light beam was kept between 300 and 800 nm with the help of mono-chromator (Oriel Model 74100). The beam was mechanically chopped at 9 Hz. The optical absorption coefficient (β) varied with the excitation light energy ($h\upsilon$) [8] and is given by the expression, $(\beta h\upsilon)^2 = C(h\upsilon - E_g)$ where $h\upsilon$ is the photon energy, C is constant and E_g is the optical energy band-gap. PPE signal intensity (ρ) is directly proportional to β, hence $(\rho h\upsilon)^2$ is related to $h\upsilon$ linearly. From the plot of $(\rho h\upsilon)^2$ versus $h\upsilon$, E_g is obtained by extrapolating the linear fitted region to zero.

Optical-absorption edge has been observed in a variety of crystalline and amorphous materials. The optical-absorption edge has important role in electron or excitone-phonon interactions [9]. It is found that PPE signal intensities plotted semi logarithmically varies linearly with the photon energy ($h\upsilon$) just lower than the fundamental absorption edge [10]. Therefore, an empirical relationship for the dependence of the PPE signal intensity on the absolute measuring temperature (T) and photon energy ($h\upsilon$), given by the equation:

$$P = P_o e^{\left[\frac{\sigma(h\upsilon - h\upsilon_O)}{KT}\right]} \quad (1)$$

where K is the Boltzman's constant and P_o, σ, υ_o are fitting parameters [11,12]. The value σ/KT, which determines the exponential slope, where σ is the steepness factor and is characterized in optical absorption edge. The steepness factor is found (σ_A, in region-A and σ_B in region-B) from the PPE spectrum.

3. Results and discussion

There were only two phases observed in XRD patterns for the samples. The major phase was hexagonal ZnO and few small peaks of Bi_2O_3 (ref. code 002-0.8-0244), Mn_3O_4 (ref. code 00-065-1209) were observed in the XRD pattern at all sintering times. The relative density of the ceramics ZnO + 0.6 Bi_2O_3 + 0.6 TiO_2 + 0.5 MnO_2 and ZnO + 1.8 Bi_2O_3 + 1.8 TiO_2 0.5 MnO_2 decreased from 89.5, 88.3 to 87.5, 87%, respectively (Figure 3). The results indicated that the pores increased with the increase of sintering time. The grain size of the ceramics ZnO + 0.6 Bi_2O_3 + 0.6 TiO_2 + 0.5 MnO_2 and ZnO + 1.8 Bi_2O_3 + 1.8 TiO_2 + 0.5 MnO_2 increased from 39.3, 48.2 to 60.5, 76.5 μm, respectively Fig. 4. This was due to Bi_2O_3 and TiO_2 as both act as a grain enhancer. EDAX results showed that the Bi_2O_3 was segregated in the grain boundaries for both ceramics combinations at all sintering times. It was found that Mn and Ti were present in the grains. This indicates that these elements are possibly substituted in the ZnO lattice as the ionic radii of Ti^{+4} (0.68 Å) Mn^{+4} (0.53 Å) are smaller than that of Zn^{+2}(0.74 Å).

Band-gap energy (E_g) decreased from 3.2 eV (pure ZnO) to 2.19 eV for the ceramic combination ZnO + 0.6 Bi_2O_3 + 0.6 TiO_2 + 0.5 MnO_2 for one and two hour sintering time and decreased to 2.16 eV when the sintering time was increased from one to four hours (Figure 5). This decrease of 1.01 eV, i.e. from 3.2 (pure ZnO) to 2.19 eV may be due to the growth of interface states produced by the combined effect of 0.6 Bi_2O_3, 0.6 TiO_2 and 0.5 MnO_2 for one hour sintering time for this ceramic combination. A small decrease in E_g from 2.19 to 2.16 eV (0.3 eV) was due to rise in the sintering time. When the value of x was increased from 0.6 to 1.8 mol%, the combination of the ceramic was as ZnO + 1.8 Bi_2O_3 + 1.8 TiO_2 + 0.5 MnO_2. The value of E_g decreased from 3.2 (pure ZnO) to 2.19 eV for one hour sintering time. This value was further reduced to 2.14 eV for the sintering time of four hours for this ceramic combination. This decrease 1.01eV was due to the growth of interface states produced by the combined effect of 1.8 Bi_2O_3, 1.8 TiO_2 and 0.5 MnO_2 for one hour sintering time. The decrease in the value of E_g was not observed with the increased value of x that was from 0.6 to 1.8 mol% for Bi_2O_3 and TiO_2 for one hour sintering time. It was expected that the saturation limit had been reached for this quantity of Bi_2O_3 and TiO_2 for one hour sintering time. So the interface states in this ceramic combination for one hour sintering time could not be produced. For this combination, with increase in sintering time, the value of E_g decreased slightly. This slight decrease (0.05 eV) was observed at the three hours of sintering time and remained constant for four hour sintering time. This indicated that the growth of interface states was limited for this sintering time and saturation limit was reached. The small decrease was due to growth of the interface states because of the substitution of Mn^{+2} ions in the ZnO lattice as well as in the grain boundaries.

The steepness factor σ_A (in A-region), which characterizes the slop of exponential optical absorption decreased with the increase of sintering time indicating the increase in PPE signal intensity for the ceramic combination ZnO + 0.6 Bi_2O_3 + 0.6 TiO_2 + 0.5 MnO_2 (Figure 6). This showed an increase in structural disordering. This structural disordering generated the interface states and correspondingly, E_g decreased in this ceramic combination (Figure 5). With the increase of x from 0.6 to 1.8 mol%, the ceramic combination was ZnO + 1.8 Bi_2O_3 + 1.8 TiO_2 + 0.5 MnO_2. The steepness factor (σ_A) also decreased for this ceramic combination. Thus showed increase in PPE signal intensity for this ceramic combination (Figure 4). This showed an increase in structural disordering. The structural disordering generated the interface states and correspondingly, E_g decreased in this ceramic combination (Figure 5) [15].

Generally an exponential tail (in region-B) for crystalline semiconductors can be characterized by

$$(\sigma_B/KT)^{-1} = A\langle U^2\rangle_T/C_o \quad (2)$$

where C_o is the exponential tail parameter of the order of unity and $\langle U^2\rangle_T$ is the thermal average of the square of the displacement of the atoms from their equilibrium positions. The term $A\langle U^2\rangle_T$ expresses the energy of the displacement of atom. [13, 14].

The steepness factor (σ_B) for the ceramic combination ZnO + 0.6 Bi_2O_3 + 0.6 TiO_2 + 0.5 MnO_2 decreased with the increase of sintering time. This indicates the increase in the thermal energy of displacement of atoms for this ceramic combination (Fig. 7). The increase in the structural disordering at the grain boundaries as well as in the grain interiors and correspondingly, the value of E_g decreased (Figure 3). The value of steepness factor (σ_B) also decreased with the increase in value of x from 0.6 to 1.8 mol% and ceramic combination was ZnO + 1.8 Bi_2O_3 + 1.8 TiO_2 + 0.5 MnO_2.

4. Conclusion

Photopyroelectric spectroscopy of doped ZnO shows growth of interface states at the grain boundaries as well as on the grain surfaces. The study also shows the occurrence of structural disordering by the Bi_2O_3 liquid phase effect.

Acknowledgements

The authors acknowledge the financial support of Ministry of Higher Education, Government of Malaysia through FRGS Project # 01-01-0739FR

References

[1] M. Caglar, Y. Caglar, S. Ilican, J. Optoelectronic. Adv. Mater. **8** (4), 1410 (2006).
[2] T. T. K. Gupta, J. Am. Ceram. Soc. **73**(7), 1817 (1990).
[3] H. M. Lin, S. J. Tzeng, P. J. Hsiau, W. L. Tsai, Nanostruct. Mater. **12**, 465 (1998).
[4] D.C. Look, Materials Science and Engineering B **80**, 383 (2001).
[5] K. Eda, IEEE Elect. Insul. Mag. **5**, 28 (1989).
[6] A. Minamide, M. Shimaguchi, Y. Tokunaga, Jpn. J. Appl Phys. **37**, 3144 (1998).
[7] A. Mandelis. Chem. Phys. Lett. **108**, 388 (1984)
[8] T. Toyoda, H. Nakanishi, S. Endo, T. Irie, J. Phys. D Appl. Phys. **18**, 747 (1985)
[9] T. Toyoda, J. Appl. Phys., **61**(1), 434. (1987)
[10] F. Urbach,. Phys. Rev. **92,** 1324 (1953)
[11] J. D. Dow, D. Redfield, Phys. Rev., **B5**, 594 (1972)
[12] S. Qing,. T. Toyoda, Jpn. J. Appl. Phys. **38**, 3163 (1999)
[13] J. Tauc, Amorphous and Liquid Semiconductors. Ed, J. Tauc.(Plenum Press London,) p.159 (1981)
[14] T. Toyoda, H. Fujimoto, T. Konaka, Jpn. J. Appl. Phys. **36,** 3292 (1997)
[15] T. Toyoda, S. Shimamoto, Jpn. J. Appl. Phys. **37,** 2827 (1998)

*Corresponding author: zahidrizwan64@gmail.com